Soft Matter

Accepted Manuscript

ROYAL SOCIETY OF CHEMISTRY

www.rsc.org/softmatter

Table of Content (TOC) of

"Multi-responsible Chameleon Molecule with Chiral Naphthyl and Azobenzene Moieties"

Dae-Yoon Kim, Sang-A Lee, Minwook Park, Yu-Jin Choi, Shin-Woong Kang, and Kwang-Un Jeong*

A newly synthesized multi-responsible chameleon molecule with chiral naphthyl and azobenzene moieties was successfully applied as a reversible modulating devices responding to the temperature, electric field and light.

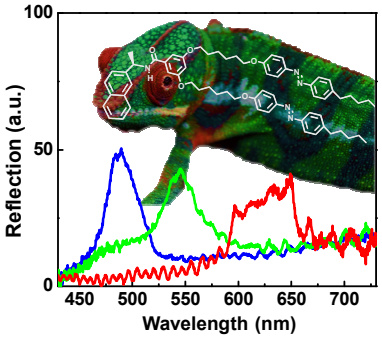

Soft Matter

RSCPublishing

ARTICLE

Multi-responsible Chameleon Molecule with Chiral Naphthyl and Azobenzene Moieties

Cite this: DOI: 10.1039/xoxxoooooox

Dae-Yoon Kim,[a] Sang-A Lee,[a] Minwook Park,[a] Yu-Jin Choi,[a] Shin-Woong Kang,[b] and Kwang-Un Jeong[a,*]

Received ooth January 2012,
Accepted ooth January 2012

DOI: 10.1039/xoxxoooooox

www.rsc.org/

A photochromic chiral molecule with the azobenzene mesogens and the (R)-configuration naphthyl moiety (abbreviated as NCA_2M) was specifically designed and synthesized for the demonstration of chameleon-like color changes responding to the multitudinous external stimuli, such as temperature, light and electric field. The basic phase transition behaviors of NCA_2M were first studied by the combination of differential scanning calorimetry (DSC) and polarized optical microscopy (POM). Based on the structure-sensitive X-ray diffraction results obtained at different temperatures, it was comprehended that the NCA_2M molecule exhibited the tilted version of highly ordered smectic crystal phase with the 5.45 nm layer thickness. Chiral nematic (N*) liquid crystals (LC) with helical superstructures were formed by doping the NCA_2M photochromic chiral molecule in an achiral nematic (N) LC medium. By controlling the helical pitch length of N*-LC with respect to temperature, light and electric field, the wavelength of selectively reflected light from the N* photonic crystal was finely tuned. The light-induced color change of N*-LC film was the most efficient method for covering the whole visible region from blue to green and to red, which allows us to fabricate the remote-controllable photo-responsive devices.

Introduction

Liquid crystals (LC) are unique soft materials showing the mobility of liquid as well as the order of crystal.[1] Calamitic nematic (N) LC exhibits the angular distribution of long molecular axis with specific direction and high symmetry.[2] Since the physical and optical properties of soft materials rely on molecular arrangements, it is essential to control their orientations on the different length scales.[3] The molecular orientation of soft materials showing the N-LC phase can be finely controlled with heat, electric field, and light.[4]

The chiral nematic (N*) LC phase, which is a chiral version of N-LC phase, possesses solely the one-dimensional long-range molecular orientational order along the long axis of N-LC molecule.[5] The N*-LC phase is well-known to exhibit optically active variants and selective reflections of light.[6] Because the N*-LC phase is readily formed by introducing chiral molecules into the achiral N-LC medium, the helical pitch length of N*-LC can be adjusted by the concentration of chiral dopant and by the helical twisting power change of chiral dopant itself.[7] When the pitch of N* structure is in the range of visible spectrum, iridescent colors can be observed with naked eyes.[8]

Therefore, the N*-LC films, which are also called as cholesteric LC (CLC) films, have attracted considerable interests not only in scientific aspects of partially ordered soft materials but also in engineering point of views of displays and optical applications.[9] There have been considerable applications for the N*-LC films of color tunable and switchable materials.[10] Generally, the reflection colors in N*-LC depend on the periodicity of the helical superstructure and the refractive index of the system which can be tuned by the external stimulations of pH, pressure, swelling, temperature, electric field and light.[11]

Among them, the photo-induced reflection color controls have unsurpassed advantages for their applications since the remote control is possible in the color-switching systems in N*-LC mixtures.[12] In this circumstance, a wide range of photo-responsive chiral dopants has been investigated including azobenzenes, spiropyrans, fulgides, overcrowded alkenes and diarylethenes.[13] The azobenzene-based chiral dopants have received intensive attentions because not only the photo-reversible *trans* ↔ *cis* molecular conformation changes can vary the helical pitch but also the cylindrical molecular shape enhances the compatibility and solubility in the N*-LC systems.[14] By simply mixing the azobenzene-based chiral dopants in the N*-LC phase, a macroscopic chirality can be easily tuned and the corresponding reflection colors are selectively controlled by the use of suitable light.[15]

In this aspect, a novel photochromic chiral molecule (abbreviated as NCA_2M) was specifically designed and synthesized by chemically attaching the azobenzene mesogens

to the naphthyl group with (R)-configuration. The photochromic azobenzene groups in the NCA_2M molecule can reversibly respond to lights, while the presence of a chiral naphthyl group provides its molecular chirality and breaks the molecular packing symmetry.[16] After studying the phase transition behaviors of NCA_2M using differential scanning calorimetry (DSC) and polarized optical microscopy (POM), the photochemical properties of the NCA_2M molecule were also investigated in common organic solvents and in a typical N*-LC medium. Furthermore, the chameleon-like color changes of the N*-LC with NCA_2M chiral dopant were demonstrated by tuning temperature, light and electric field.

Experimental section

Materials.

4-pentyl aniline (98%, Aldrich), phenol (99%, Aldrich), 1,6-dibromohexane (96%, Aldrich), methyl 3,5-dihydroxybenzoate (DHB, 98%, Aldrich), *N*-(3-dimethylaminopropyl)-*N*′-ethylcarbodiimide hydrochloride (EDC, 99%, Aldrich), 4-(dimethylamino)pyridine (DMAP, 99%, Aldrich), (R)-1-(2-naphthyl)ethylamine (CNE, 99%, Aldrich), anhydrous butanone (99%, Sigma-Aldrich), anhydrous chloroform (99%, Sigma-Aldrich), absolute ethanol (99.5%, Sigma-Aldrich), hydrochloric acid (HCl, 37%, Sigma-Aldrich), sodium hydroxide (NaOH, 93%, Showa), sodium nitrite ($NaNO_2$, 97%, Showa), potassium carbonate (K_2CO_3, 99%, Showa), anhydrous magnesium sulphate ($MgSO_4$, 99.5%, Showa), chiral dopant (R-811, Merck Co.) and achiral nematic liquid crystal (N-LC, MLC 15600-100, Merck Co.) were used as received.

Synthesis.

4-(4-pentylphenylazo)phenol (1). A solution of 4-pentylaniline (8.1 g, 50 mmol) and HCl (15 mL) in water (100 mL) was cooled at 0 °C and $NaNO_2$ (3.5 g, 50 mmol) was slowly added in small portions by maintaining the temperature below 5 °C. After stirring for 1 h, the solution of the diazonium salt was added to a cold solution of phenol (4.7 g, 50 mmol) and NaOH (2.5 g in 25 mL water). Here, the temperature was kept below 5 °C. The product was precipitated by the addition of small portion of NaCl. By recrystallization of the product in ethanol, the purified reddish crystal was collected (yield: 71%, 9.5 g). ^{1}H NMR (400 MHz, DMSO-*d*): δ = 10.2 (s, 1H), 7.76 (d, 2H), 7.72 (d, 2H), 7.35 (d, 2H), 6.92 (d, 2H), 2.64 (t, 2H), 1.60 (m, 2H), 1.29 (m, 4H), 0.85 ppm (t, 3H).

4-(6-bromohexyloxy)phenyl-(4-pentylphenyl)diazene (2). A mixture of **1** (5.0 g, 20 mmol), 1,6-dibromohexane (24.4 g, 100 mmol), K_2CO_3 (5.9 g, 36 mmol) and butanone (150 mL) was stirred and heated to reflux for 24 h. After the reaction, the solvent was removed in vacuum and the residue was dissolved in chloroform and extracted with distilled water several times. Yellow crystals were obtained by recrystallization of the crude oil in methanol and acetone (yield: 76%, 6.1 g). ^{1}H NMR (400 MHz, $CDCl_3$): δ = 7.89 (d, 2H), 7.80 (d, 2H), 7.30 (d, 2H), 7.00 (d, 2H), 4.04 (t, 2H), 3.43 (t, 2H), 2.67 (t, 2H), 1.91 (m, 2H), 1.82 (m, 2H), 1.65 (m, 2H), 1.55 (m, 4H), 1.34 (m, 4H), 0.89 ppm (t, 3H).

3,5-bis[6-(4-(4-pentylphenylazo)phenoxy)hexyloxy]-benzoic acid ethyl ester (3). A mixture of **2** (4.29 g, 10.0 mmol), DHB (0.60 g, 3.0 mmol), K_2CO_3 (2.10 g, 15.2 mmol), KI (0.02 g, 0.15 mmol), and butanone (50 mL) was heated to reflux for 48 h. After the reaction, solvent was removed in vacuum and the residue was re-dissolved in chloroform and washed with distilled water three times. It was purified by column chromatography with silica gel by using ethyl acetate:chloroform = 1:20 and subsequent recrystallization with methanol. The resulting product was a yellowish solid (yield: 55%, 1.7 g). ^{1}H NMR (400 MHz, $CDCl_3$): δ = 7.89 (d, 4H), 7.78 (d, 4H), 7.72 (d, 4H), 7.16 (d, 2H), 6.98 (s, 4H), 6.64 (s, 1H), 4.04 (t, 4H), 3.99 (t, 4H), 3.89 (s, 3H), 2.66 (t, 4H), 1.84 (m, 8H), 1.65 (m, 4H), 1.55 (m, 8H), 1.34 (m, 8H), 0.89 ppm (t, 6H).

3,5-bis[6-(4-(4-pentylphenylazo)phenoxy)hexyloxy]benzoic acid (4). Aqueous KOH (10 M, 10 mL) was added to a stirred solution of **3** (0.5 g, 0.57 mmol) in ethanol (50 mL). The mixture was heated at reflux for 3 h, and then neutralized with an HCl to obtain a precipitate. The precipitate was filtered off and washed with water. The crude product was purified by reprecipitation from chloroform and ethanol, and dried under vacuum to afford **4** as a yellow solid (yield: 93%, 0.45 g). ^{1}H NMR (400 MHz, $CDCl_3$): δ = 7.89 (d, 4H), 7.78 (d, 4H), 7.72 (d, 4H), 7.16 (d, 2H), 6.98 (s, 4H), 6.64 (s, 1H), 4.04 (t, 4H), 3.99 (t, 4H), 2.66 (t, 4H), 1.84 (m, 8H), 1.65 (m, 4H), 1.55 (m, 8H), 1.34 (m, 8H), 0.89 ppm (t, 6H).

NCA_2M (5). EDC (0.3 g, 1.56 mmol) and DMAP (0.2 g, 1.64 mmol) were added to a solution of **4** (0.3 g, 0.35 mmol) in anhydrous chloroform (30 mL). After stirring at room temperature for 30 min, chiral naphthyl ethylamine (0.19 g, 1.11 mmol) was added as a solid. The solution was stirred for 24 h at room temperature. After the reaction, distilled water was added and the product was extracted with chloroform. The combined organic layer was dried over anhydrous $MgSO_4$. After filtration and evaporation, the crude product was purified by column chromatography with silica gel using ethyl acetate:methylene chloride = 1:20 to yield **5** as an orange powder (yield: 77%, 0.27 g). ^{1}H NMR (400 MHz, $CDCl_3$): δ = 7.89 (d, 4H), 7.84 (m, 4H), 7.78 (d, 4H), 7.48 (m, 3H), 7.72 (d, 4H), 6.98 (d, 4H), 6.88 (d, 2H), 6.64 (s, 1H), 5.47 (m, 1H), 4.04 (t, 4H), 3.99 (t, 4H), 2.66 (t, 4H), 1.84 (m, 11H), 1.67 (m, 4H), 1.55 (m, 8H), 1.34 (m, 8H), 0.89 ppm(t, 6H). ^{13}C NMR (400 MHz, $CDCl_3$): δ = 166.4, 161.3, 160.3, 151.0, 146.9, 145.7, 140.4, 136.7, 133.3, 132.8, 129.0, 128.5, 127.9, 127.6, 126.2, 125.9, 124.7, 124.5, 122.5, 114.6, 105.3, 104.2, 68.1, 49.3, 35.8, 31.4, 30.9, 29.1, 25.8, 22.5, 21.5, 14.0 ppm. MS (MALDI-ToF) for m/z calcd 1008.34; $[M+Na]^+$ found: 1031.23. Elemental analysis calcd (%) for $C_{65}H_{77}N_5O_5$: C 77.42 H 7.70 N 6.95 O 7.93; found: C 77.06 H 7.71 N 6.94.

Characterization.

Proton (^{1}H) and carbon-13 (^{13}C) nuclear magnetic resonance (NMR) spectra were recorded on a JNMEX400 spectrometer in

deuterated chloroform ($CDCl_3$). Matrix assisted laser desorption ionization time-of-flight mass spectroscopy (MALDI-ToF MS, Voyager-DE STR Biospectrometry Workstation) and elemental analysis (Vario EL) experiments were conducted to identify the chemical structure and purity. The ultraviolet-visible (UV-Vis) absorption spectra in chloroform solution was measured by the UV-Vis spectrophotometer (Jasco, ARSN-733). Optical switching behaviors were characterized by fiber-optic spectrophotometer (Ocean Optics, QP1000) equipped with reflection mode of optical microscopy. Additionally, the Cerius^2 simulation software from Accelrys (version 4.6) was used to calculate the minimal-energy geometry in the isolated gas-phase utilizing the COMPASS force field.

The thermal behavior was monitored by using a PerkinElmer PYRIS Diamond differential scanning calorimetry (DSC) equipped with an Intracooler 2P apparatus. The transition temperatures were determined by measuring the onset temperatures obtained during the cooling and heating scans. The change of optical textures at a given temperature was observed by using cross-polarized optical microscopy (POM, Nikon ECLIPSE E600POL) coupled with a LINKAM LTS 350 heating stage.

One-dimensional (1D) wide-angle X-ray diffraction (WAXD) experiments were conducted using Rigaku 12 kW rotating-anode X-ray (CuKα radiation) generator coupled with a diffractometer. The diffraction peak positions and widths were calibrated with silicon crystals. Samples were scanned across a 2θ-angle range of 1.5° to 35° at a scanning rate of 2° min^{-1}. The 2D WAXD patterns were obtained using a Rigaku X-ray imaging system with an 18 kW rotating anode X-ray generator. Silicon crystal powder, used as an internal reference, shows a diffraction ring at a 2θ value of 28.466°. For the 2D WAXD experiment, at least 10 min of exposure time was required for a high-quality pattern. In both 1D and 2D WAXD experiments, background scatterings were subtracted from the sample scans.

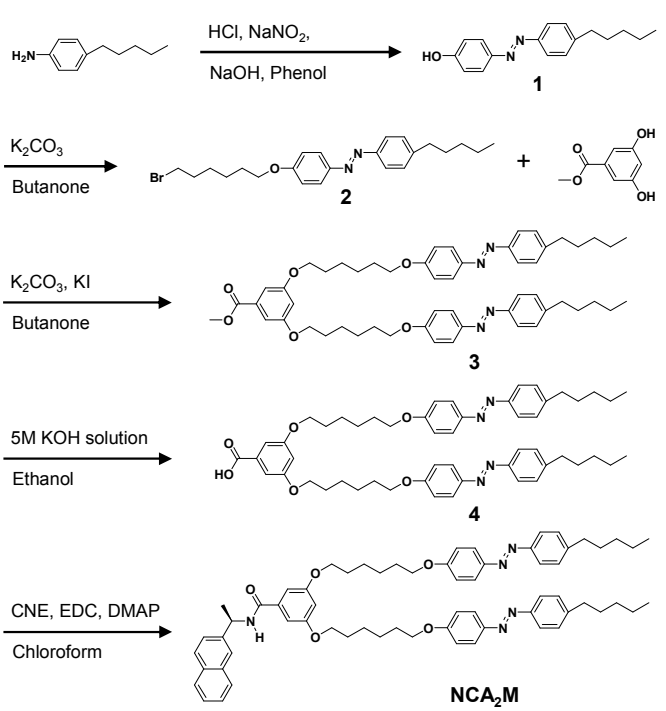

Scheme 1. Synthetic procedures of photo-responsive chiral molecule, NCA_2M.

Result and discussion

Programmed photochromic chiral molecule

As illustrated in Scheme 1, a naphthalene-based chiral molecule (abbreviated as NCA_2M) containing two azobenzene mesogens with alkyl chains is newly designed and synthesized. The detailed synthetic procedures are explained in the Experimental section of this paper. The NCA_2M molecule is obtained by the amidation coupling reaction of chiral naphthyl ethylamine with two *trans*-azobenzene derivatives in the presence of EDC and DMAP. The azobenzene derivatives are specifically introduced for the photochromic groups to increase the compatibility between NCA_2M and N-LC host medium. Furthermore, the hydrophobic alkyl chains covalently connecting to the both side of azobenzene and the di-hydroxybenzoate (DHB) group also enhance the compatibility with N-LC.[17]

Since the photochromic azobenzene moiety is applied as the mesogenic group in NCA_2M, the molecular conformations and phase structures can be reversibly switched with respect to temperature and light.[18] Here, the naphthyl group is specifically chosen for the chiral core, because the chiral compound derived from naphthyl ethylamine are effective for breaking the molecular packing symmetries within the N-LC media.[19] The target compounds are purified by column chromatography. Chemical structures and purities of NCA_2M and its intermediates are confirmed by thin-layer chromatography (TLC), ^{1}H NMR spectroscopy (see Figs. S1-S5 in the Electronic Supplementary Information), ^{13}C NMR spectroscopy (Fig. S6), MALDI-ToF (Fig. S7) and elemental analysis (Fig. S8).

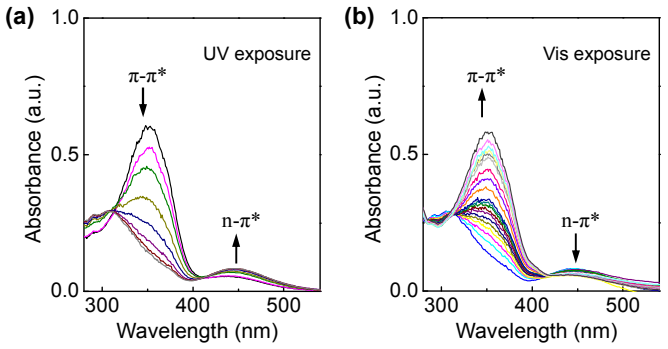

Figure 1. UV-Vis absorption spectra of NCA_2M by irradiating (a) 365 nm and (b) 450 nm light, respectively.

In order to investigate the absorption properties of the NCA_2M compounds, UV-Vis absorption measurements in chloroform solution (2×10^{-2} mM) are conducted. As indicated in Fig. 1a, the absorption band between two isosbestic points (312 and 412 nm) corresponding to the π-π* transition is originated from the *trans*-form of azobenzene, whereas the ground state (n) of the *cis* conformer of azobenzene is excited to the π* state by absorbing the UV-light in the range of 410-540 nm. As shown in Fig. 2a, upon irradiating the UV-light with a maximum intensity at 365 nm, the thermodynamically stable *trans* conformer of azobenzene transforms to its metastable *cis* conformer and reaches into a new photo-stationary state ($PSS_{365\ nm}$) in 60 s (Fig. 2a). On the other hand, as subsequently irradiating Vis-light (450 nm), the amount of *trans* conformational azobenzene isomer is increased by concomitantly decreasing the intensity and area of the absorption band for the *trans*/*cis* isomers of azobenzene (Fig. 1b). Absorption bands recover the initial state ($PSS_{450\ nm}$) after 60 min (Fig. 2b). Photo-isomerization rate constants of π-π* and n-π* transitions are $K_t = 6.72 \times 10^{-2}$ s^{-1} and $K_c = 9.78 \times 10^{-2}$ min^{-1}, respectively (Fig. S9). Transition between two photo-stationary states is a fully reversible process by alternating UV- and Vis-light irradiations, which allows us to fabricate a reversible photo-modulating device.[20]

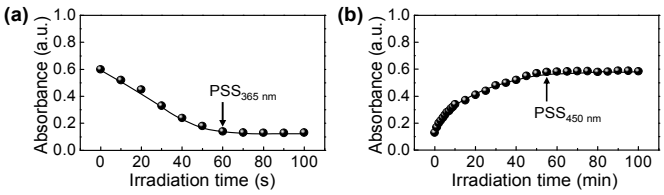

Figure 2. Absorbance at 365 nm of NCA_2M in chloroform at room temperature under (a) UV light for 100 s and (b) Vis light for 100 min, respectively

Thermodynamic transition and its corresponding structural evolution of NCA_2M molecule

To determine the thermal transition temperature and quantitative thermodynamic properties of the NCA_2M compound, DSC experiment is conducted.[21] As shown in Fig. 3, DSC thermograms exhibit a single exothermic peak at different cooling rates from 2.5 to 20 °C min^{-1} in the investigated temperature range. Upon increasing the cooling rate, the onset temperature shifts to lower temperatures and the heat (ΔH) release at transition is reduced. At the 2.5 °C min^{-1} cooling rate, the onset temperature of the exothermic transition and corresponding heat are 94.2 °C and -36.7 J g^{-1} (-37.0 kJ mol^{-1}), respectively, which are reduced to 85.7 °C and -33.1 J g^{-1} (-33.4 kJ mol^{-1}) at 20 °C min^{-1}. From the linear dependence on the cooling rate, the onset transition temperature and heat at equilibrium are estimated to be 95 °C and -37 kJ mol^{-1}, respectively. The variation of the transition temperature depending on the cooling rate implies that the heat is associated with crystallization.[22] Hence, the endothermic thermal transition detected upon subsequent heating is ascribed to the crystal melting. The thermodynamic properties obtained from the subsequent heating process are consistent with those from the cooling process.

Although the DSC technique is sensitive to heat absorption and release events at thermal transitions and serves quantitative thermodynamic properties, it does not provide direct information regarding the molecular order at transitions.[23] 1D WAXD is used to investigate the temperature-dependent structural development of NCA_2M. Fig. 4b shows a set of 1D WAXD patterns of the NCA_2M compound obtained at a cooling rate of 2.5 °C min^{-1}. Above 95 °C, the NCA_2M molecules are in the isotropic state (I), exhibiting only two amorphous halos at 2θ = 2.25° (d-spacing = 3.93 nm) and 2θ = 19.38° (d-spacing = 0.45 nm), which correspond to the average periodicity of electron density fluctuations among the nanophase-separated NCA_2M and to the average distance between the amorphous mesogens, respectively. The isotropic melt above T_i was further confirmed by the observation of the complete dark state at 120 °C under the polarized optical microscopy (POM) due to the crystal melting.

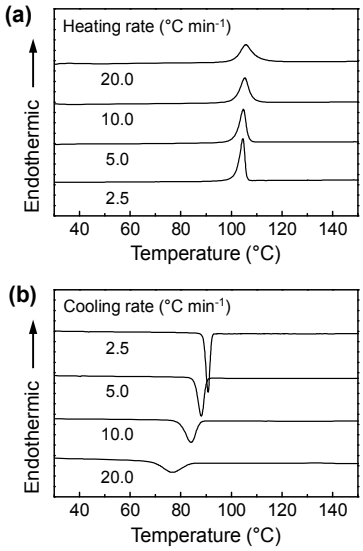

Figure 3. Sets of DSC heating (a) and cooling (b) thermal diagrams for NCA_2M at different scanning rates ranging from 2.5 to 20 °C min^{-1}.

Just below the isotropization temperature (T_i = 95 °C), five apparent low-angle reflections at 2θ = 1.62° (d = 5.45 nm), 2θ = 3.33° (d = 2.65 nm), 2θ = 4.89° (d = 1.80 nm), 2θ = 6.51° (d = 1.35 nm) and 2θ = 8.12° (d = 1.08 nm) start to develop. In addition to the changes of the low 2θ-angle region, a sudden narrowing of the high 2θ-scattering halo occurs at 2θ = 17.93°, 21.19° and 23.03°, which their corresponding d-spacings are 0.49, 0.42 and 0.38 nm, respectively. This result means that the highly ordered phase is emerged. The formation of highly ordered phase is also monitored under POM at 30 °C, as shown in Fig. 4a. Therefore, based on the POM results combined with those of DSC and 1D WAXD, it is realized that there is one ordered phase below the T_i = 95 °C.

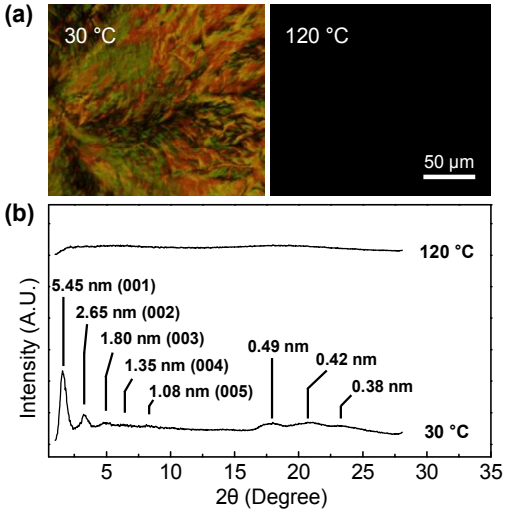

Figure 4. (a) POM images of NCA_2M during the cooling process; (b) 1D WAXD patterns at different temperatures.

Identification of molecular packing structure of NCA_2M molecule

To obtain the structural and symmetry information of the ordered phase in detail, 2D WAXD experiment from the oriented NCA_2M samples must be conducted.[24] Fig. 5a shows the 2D WAXD pattern of an oriented NCA_2M sample. The macroscopically oriented NCA_2M sample is prepared by mechanically shearing at 90 °C and subsequent annealing by a slow cooling from 90 °C to room temperature. The incident X-ray beam direction is perpendicular to the shear direction (SD, parallel to the equator). Diffraction arc positions and widths in Fig. 5a are calibrated based on the diffraction ring of silicon power crystal at 2θ = 28.466° (d = 0.314 nm). In this 2D WAXD pattern, diffraction information of NCA_2M molecular arrangements appears on two different length scales. One is on the nanometer length scale in the low 2θ-angle region between 1.5° and 10°, in which the self-assembled information for layered structure of NCA_2M can be obtained. Diffractions on the sub-nanometer length scale between 10° and 30° can provide information about the lateral molecular packing structures between the nanophase separated azobenzene mesogens and naphthyl groups.

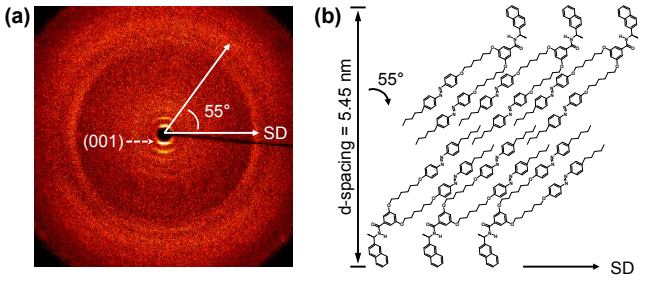

Figure 5. 2D WAXD pattern of the crystalline phase of NCA2M at room temperature (a) and molecular packing models in the crystalline phase (b)

In Fig. 5a, a strong diffraction at 2θ = 1.62° (d = 5.45 nm) is detected on the meridian with its high order diffractions at 2θ = 3.33° (d = 2.65 nm), 2θ = 4.89° (d = 1.80 nm), 2θ = 6.51° (d = 1.35 nm), 2θ = 8.12° (d = 1.08 nm), 2θ = 17.93° (d = 0.49 nm) and 2θ = 21.19° (d = 0.42 nm). This result indicates that the highly ordered structure of NCA_2M is a basically layer structure with the layer d-spacing of 5.45 nm. Therefore, Miller indices of the diffractions at 2θ = 1.62°, 3.33°, 4.89°, 6.51°, 8.12°, 17.93° and 21.19° are identified as (001), (002), (003), (004), (005), (0011) and (0013), respectively. However, based on the global equilibrium geometry of NCA_2M calculated at 0 K utilizing the COMPASS force field of Cerius^2 4.6 software, the theoretical length of NCA_2M is 3.41 nm (Fig. S10). Although the calculation is based on the all-*trans* conformation of alkyl and azobenzene groups, the calculated molecular length (*l*) is significantly smaller than the detected layer spacing (d). Note that the bigger layer spacing of NCA_2M molecule indicates that a bilayer structure is formed with an interdigitation and the constructed bilayer building block is tilted away from the layer normal.[25] The reflection in the quadrant at 2θ = 23.03° (d = 0.38 nm) is found 35° away from the meridian (layer normal direction). This diffraction result clearly indicates that the bilayered and interdigitated NCA_2M building blocks are tilted 55° away from the layer normal direction, as schematically illustrated in Fig. 5b. Note that the scattering halo detected at 2θ = 23.03° in the quadrant is originated from the average periodicity of electron density fluctuations between the nanophase separated azobenzene mesogens with a tilted arrangement. On the equator of 2D WAXD along the SD, a pair of diffraction arcs is detected at 2θ = 17.93° (d = 0.49 nm). Diffractions on the equator as well as in the quadrants in the wide angle region means that a highly ordered structure is formed in the 3D by the lateral molecular close packing. Even though the quality of 2D WAXD pattern is not excellent and the diffraction information is limited, it is obvious that the NCA_2M molecule are self-assembled to make the bilayer building blocks which are further laterally self-organized with tilted fashion in the layered superstructure. To understand more detail molecular packing structure of NCA_2M compound, this 2D WAXD result should be analyzed by the support of the electron diffractions of single crystals and the computer simulations in the real and reciprocal spaces.

Temperature-dependent color change of N*-LC film

The mixtures of N-LC medium with a chiral dopant selectively reflect different colors according to the Bragg's law, $\lambda_{max} = n \times p$, where λ_{max} is the centre wavelength for the maximally reflected light, n is the refraction index of LC, and p is the helical pitch in micrometres.[26] However, to realize its potential in the practical applications for optical devices, the reflection band of N*-LC film is required to be in visible wavelength. It is noteworthy to remind that the pitch length can be controlled by tuning the concentration of the chiral dopant with different handedness.[27] In this research, two chiral molecules with (R)-configuration are used to induce N*-LC phase: one is a laboratory synthesized novel chiral naphthyl NCA_2M molecule with photo-responsive azobenzene group and the other is a commercially available chiral dopant (R)-811 bearing high helical twisting power. By simply dissolving the chiral molecules in the N-LC host, the N*-LC mixtures are prepared and loaded into standard electro-optic cells.

For example, the N*-LC mixtures of 1.0 wt% of NCA_2M and 29.0 wt% of (R)-811 in N-LC host MLC 15600-100 are capillary-filled into a 10 μm thick glass cell coated with polyimide planar alignment layer (see Fig. 6). The aligned N*-LC texture is observed at room temperature under POM (Fig. 7a). As expected, a characteristic oily-streak texture for the N*-LC phase is observed. By adjusting the chiral concentration, the pitch length of the N*-LC mixture is optimized to reflect colors in the visible region. At the initial state, as shown in Figs. 7a and 7d, the cell exhibits a reflection band at *ca.* 480 nm at room temperature. Fig. 7d shows the temperature dependence of selective reflections measured during the heating process.

As seen in Fig. 7d, the wavelength of the reflection peak is red-shifted by increasing temperature while the reflection efficiency decreases with temperature. It is obvious that the cholesteric pitch increases with temperature, indicating that the helical twisting power (HTP) of the chiral additive is inversely proposal to temperature. Although the mixture retains its cholesteric phase at the temperature above 55 °C up to the T_{NI} (63 °C), the N*-LC film does not show any characteristic reflection band in the visible region. It is likely due to the extended helical pitch to the longer wavelengths and the consequently limited the repetition of helical twist at the fixed layer thickness. As seen in Fig. 7c, the oily streaks are completely absent and no strong reflection band is observed in the entire spectral range. The helical twisting power of chiral molecules abruptly decreases during the phase transition from cholesteric to isotropic phases.[28]

Nematic liquid crystal: MLC15600-100 (Merck Co.)

Chiral dopant: (R)-811 (Merck Co.)

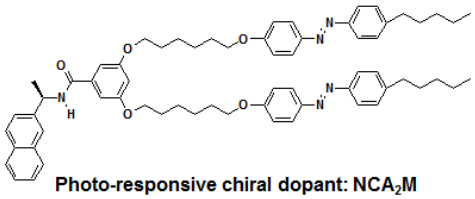

Photo-responsive chiral dopant: NCA_2M

	NCA_2M	(R)-811	N-LC
Composition	1.0 wt%	29.0 wt%	70.0 wt%

Figure 6. Materials information: host nematic liquid crystal (N-LC) MLC 15600-100, chiral dopant (R)-811, NCA_2M molecule and their weight ratio in the mixture.

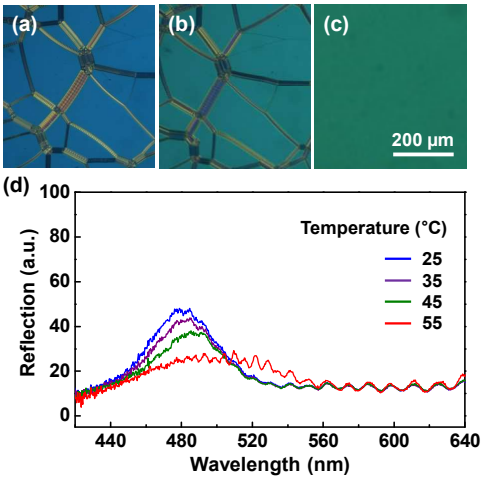

Figure 7. POM images of the N*-LC phase of the 1.0 wt% NCA_2M with 29.0 wt% (R)-811 in N-LC host at 25 °C (a), 55 °C (b), 60 °C (c), and their spectral change in the selective reflection, caused by temperature change (d).

Spectral shift of selective reflection under electric fields

To investigate an electric field induced reflection shift, the N*-LC mixtures are filled into the 10 μm thick electro-optic cell with planar anchoring boundaries. At first, to understand switching behaviors of the N*-LC under applied voltages, the electro-optic measurements have been carried out at the room temperature. Fig. 8a presents the POM images of N*-LC imposed by various amplitudes of square wave voltages at 1.0 kHz. The initial state exhibits characteristic planar texture with oily streaks as seen in Fig. 8a. Without the electric field, the reflection of the cell corresponds to blue color with a reflection maximum around 480 nm (Fig. 7 and Fig. 8). As the voltage is increased above 15 V_{pp}, the planar texture transforms to the focal conic (FC) state. At 80 V_{pp}, the cholesteric helix is completely unwound and the light-scattering FC state turns to transparent homeotropic state (Fig. 8). The dark POM image and conoscopic figure in the inset clearly show that the cholesteric helix is unwound and the uniaxial optic axis is aligned perpendicular to the substrate plane (*i.e.,* homeotropic

state). Since no significant reflection from N*-LC film is observed above 15 V_{pp}, the spectral shift for selective reflection has been investigated as a function of applied voltage prior to the transition to FC state.

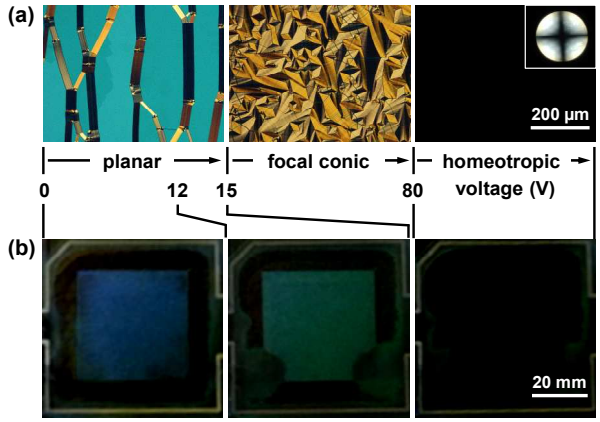

Figure 8. POM images of electric field induced state for the 1.0 wt% NCA_2M with 29.0 wt% (R)-811 in N-LC host (a) and their corresponding real cell images (b).

Fig. 9 presents the spectral shift controlled by external electric field in the planar state. No significant change has been observed below 12 V_{pp}. However, reflection band sensitively responds to the external field in the range from 12 to 15 V_{pp}. The initial blue reflection at 480 nm shifts to green at 530 nm as seen in Fig 8b and Fig 9. The inset in Fig. 9 shows conspicuous broadening and weakening of selective reflection. These characteristics are attributed to the reorientation of LC molecules and subsequent deformation of the cholesteric helix. With the increase of applied electric field, LC molecules with positive dielectric anisotropy ($\Delta\varepsilon > 0$) begin to rotate for a minimized dielectric energy. Therefore, LC molecules initially on the plane of substrates partially tilt toward substrate normal (*i.e.*, parallel to the applied electric field). Consequently, the cholesteric helix is slightly deformed by retaining the average helical axis normal to the substrate. This results in a red shift of reflection due to an oblique reflection and a gradual broadening of the reflection band.[29] Above 15 V_{pp}, however, the cholesteric helix is completely frustrated and thus turns to a light-scattering FC state as in Fig. 8a (center). As seen in the middle of Fig. 8b, the green reflection at 530 nm is originated from the tilting of a cholesteric helix from the layer normal.[24] The colors between blue and green reflection can be reversibly and continuously manipulated by tuning the applied voltage from 10 to 15 V_{pp}.

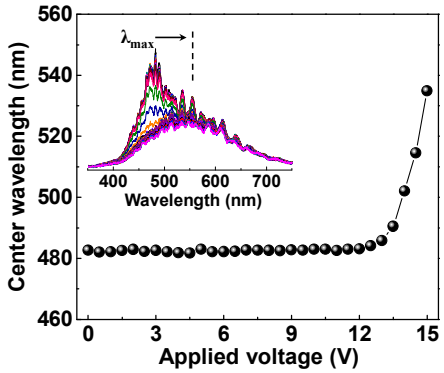

Figure 9. Center of reflection wavelength versus applied voltage obtained from the 1.0 wt% NCA_2M and 29.0 wt% (R)-811 in N-LC host at room temperature. The inset shows the measured reflection spectra under different voltages.

Remote-controlled reflection lights of N*-LC film by light

Since the NCA_2M chiral additive contains azobenzene moieties (see Scheme 1), photochromic isomerization can be easily facilitated by irradiating either UV-light for *trans*- to *cis*-isomerization or Vis-light for *cis*- to *trans*-isomerization (see Figs. 1 and 2). It is well understood that HTP is sensitively affected by chemical conformations of chiral additive.[30] It is also known that the photo-responsive chiral materials can be adopted for the manipulation of cholesteric pitch.[31] Therefore, it may be possible to reversibly change the reflected colors of N*-LC film. The LC cells with 10 μm thickness are prepared by loading the mixture with 1.0 wt% NCA_2M and 29.0 wt% (R)-811 in N-LC host. The inner surfaces of cells are treated by rubbed polyimide for a homogeneous alignment. The cells are covered with black paint on one side and placed under 365 nm UV-light illumination.

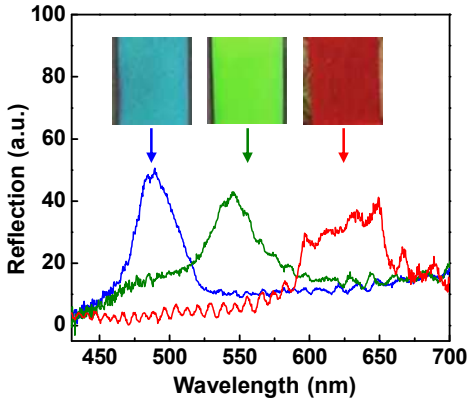

Figure 10. Macroscopic cell images and corresponding reflection spectra of the cell with 1.0 wt% NCA_2M and 29.0 wt% (R)-811 in N-LC host upon UV-irradiation at 365 nm for 0 s (blue), 5 s (green) and 10 s (red), respectively.

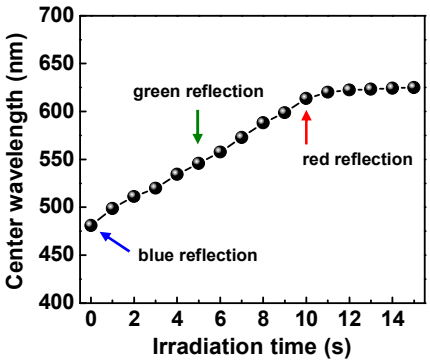

Figure 11. The spectral shift of selective reflections for the cell with 1.0 wt% NCA_2M and 29.0 wt% (R)-811 in N-LC host under continuous UV-irradiation.

Initially, a strong blue (B) reflection peaked at ~ 480 nm is observed prior to UV-light illumination as shown in Fig. 10. Upon irradiating 365 nm UV-light with the intensity of 100 mW cm^{-2}, the reflection color shifts to green (G) at ~ 545 nm in 5 s. The prolonged illumination further shifts a reflection band toward longer wavelengths and eventually the reflection saturates in red (R, ~ 620 nm) as shown in Figs. 10 and 11. At the given condition, the spectral change reaches in the equilibrium state approximately in 10 s of UV-illumination (see Fig. 11). The saturation of color shift occurs likely due to a photo-stationary state of the isomerization. Therefore, the saturation wavelength and time may be further adjusted by controlling conditions such as the irradiation intensity and the content of chiral dopant. In the absence of UV-illumination, a reflection color gradually blue-shifts and restores its pristine blue color within 20 s. The results evidently show the reversible color tuning, manipulated by external light. These observations are mainly attributed to the photochromic isomerization of chiral additive. As a result of *trans*- to *cis*- isomerization, HTP of the chiral dopant decreases significantly and the subsequent lengthening of cholesteric pitch results in a continuous red-shift of spectral reflection as a function of irradiation time. In addition, the broadening of reflection bands is evident during the spectral shift of selective reflection as seen in Fig. 10. This can be understood by the intensity dependent photo-stationary state of isomerization. Since the chiral NCA_2M molecule strongly absorb UV-light, the effective irradiation intensity for *trans*- to *cis*-isomerization depends on the penetration depth of UV-light. UV-light intensity exponentially decays as the path-length increases in the LC medium. As a result, the population of *cis*-isomer with a lower HTP is higher near UV-side, compared to far UV-side. This population gradient of isomers and corresponding HTP gradient along UV-propagation direction create subsequent pitch distribution. This eventually instigates a broadening of reflection band as observed in Fig. 10.[32]

Although the reflected colors of N*-LC can be controlled by the external stimuli, such as temperature and electric field, the range of wavelength is rather limited. At conditions for these given above, the color shift cannot cover the whole spectral range of visible light. Among those external stimuli used for the manipulation of reflection wavelength, however, the light-induced control is most attractive for practical applications since it provides full-range coverage in visible wavelengths with a reversible spectral control for the selective reflection.

Conclusions

The naphthalene-based chiral molecule (abbreviated as NCA_2M) containing two photochromic azobenzene mesogens was newly designed and synthesized. From the structure-sensitive X-ray diffraction results combined with thermal and morphological observations, it was recognized that NCA_2M formed a tilted version of highly ordered smectic crystal phase with a layered structure. Since NCA_2M molecule exhibited a good solubility in typical N-LC media, the NCA_2M can be a promising photo-responsive chiral dopant. The reflection colors from the N*-LC phase were reversibly tuned by external multi-stimuli, such as temperature, electric field, and light. A consequence of red-shift in reflected light by heat should be related to the temperature-dependent variation of the configuration of chirality, while the electric field induced red-shift in reflection band is attributed to the field induced reorientation of the N*-LC domain leading to the destruction of phase periodicity along the optical axis. By doping a photo-chemically responding chiral NCA_2M molecule, the full reflection colors (RGB) of N*-LC film were precisely tuned by changing the pitch length of the spontaneously formed helical superstructure. The multi-responsible chameleon molecule with chiral naphthyl and azobenzene moieties may allow us fabricate the reversible modulating devices responding to the temperature, electric field and light.

Acknowledgements

This work was mainly supported by the Basic Science Research Program (2013R1A1A2007238), SW Fusion Components R&D Program (MOTIE-10047806), KIST institutional program (2Z04320) and BK21 Plus Program, Korea. D.-Y.K. appreciates the support from Global Ph.D. Fellowship Program.

Notes and references

[a] Polymer Materials Fusion Research Center & Department of Polymer-Nano Science and Technology, Chonbuk National University, Jeonju, Jeonbuk, 561-756, Korea. E-mail: kujeong@jbnu.ac.kr.
[b] Department of BIN Fusion Technology, Chonbuk National University, Jeonju, Jeonbuk, 561-756, Korea.

Electronic Supplementary Information (ESI) available: ^{1}H NMR, ^{13}C NMR, MALDI-ToF, elemental analysis and detailed experimental procedures. See DOI: 10.1039/b000000x/

1. C. Tschierske, *Chem. Soc. Rev.*, 2007, **36**, 1930; L. Cseh and G. H. Mehl, *J. Am. Chem. Soc.*, 2006, **128**, 13376.
2. Q. Liu, Y. Yuan and I. I. Smalyukh, *Nano Lett.*, 2014, **14**, 4071; M. Alaasar, M. Prehm, M. Brautzsch and C. Tschierske, *Soft Matter*, 2014, **10**, 7285.
3. M. Park, Y.-J. Choi, D.-Y. Kim, S.-H. Hwnag and K.-U. Jeong, *Cryst. Growth Des.*, 2015, **15**, 900; S. Yamane, Y. Sagara and T.

Kato, *Chem. Commun.*, 2009, 3597; S. Diring, F. Camerel, B. Donnio, T. Dintzer, S. Toffanin, R. Capelli, M. Muccini and R. Ziessel, *J. Am. Chem. Soc.*, 2009, **131**, 18177.

4. X. Tong, Y. Zhao, B.-K. An and S. Y. Park, *Adv. Funct. Mater.*, 2006, **16**, 1799; A. M. Kendhale, A. P. H. J. Schenning and M. G. Debije, *J. Mater. Chem. A*, 2013, **1**, 229; D.-Y. Kim, S.-A Lee, M. Park and K.-U. Jeong, *Chem. Eur. J.*, 2015, **21**, 545; I. M. Saez and J. W. Goodby, *Chem. Commun*, 2003, 1726.
5. N. P. M. Huck, W. R. Jager, B. de Lange and B. L. Feringa, *Science*, 1996, **273**, 1686; M. Goh, S. Matsushita and K. Akagi, *Chem. Soc. Rev.*, 2010, **39**, 2466; Q. Li, L. Green, N. Venkataraman, I. Shiyanovskaya, A. Khan, A. Urbas and J. W. Doane, *J. Am. Chem. Soc.*, 2007, **129**, 12908; S. A. Cazzell, M. E. McConney, V. P. Tondiglia, L. V. Natarajan, T. J. Bunning and T. J. White, *J. Mater. Chem. C*, 2014, **2**, 132.
6. I. Dierking, *Textures of Liquid Crystals*, Wiley-VCH, Weinheim, 2003; D. J. Gardiner, W.-K. Hsiao, S. M. Morris, P. J. W. Hands, T. D. Wilkinson, I. M. Hutchings and H. J. Coles, *Soft Matter*, 2012, **8**, 9977; Y. Li, M. Wang, T. J. White, T. J. Bunning and Q. Li, *Angew. Chem. Int. Ed.*, 2013, **52**, 8925.
7. S. Shin, M. Park, J. K. Cho, J. Char, M. Gong and K.-U. Jeong, *Mol. Cryst. Liq. Cryst*, 2011, **534**, 19; C. Ruslim and K. Ichimura, *J. Mater. Chem.*, 2002, **12**, 3377; S. Kim, S.-W. Kang and K.-U. Jeong, *Soft Matter*, 2012, **8**, 9761.
8. S. H. Chen, D. Katsis, A. W. Schmid, J. C. Mastrangelo, T. Tsutsui, and T. N. Blanton, *Nature*, 1999, **397**, 506; M. E. McConney, V. P. Tandiglia, L. V. Natarajan, K. M. Lee, T. J. White and T. J. Bunning, *Adv. Optical Mater.*, 2013, **1**, 417.
9. K. M. Lee, V. P. Tondiglia, M. E. McConney, L. V. Natarajan, T. J. Bunning and T. J. White, *ACS Photonics*, 2014, **1**, 1033; A. M. Hikmet and J. Lub, *Prog. Polym. Sci.*, 1996, **21**, 1165; V. Shibaev, A. Bobrovsky and N. Boiko, *Prog. Polym. Sci.*, 2003, **28**, 729; M. Schadt, H. Seiberle and A. Schuster, *Nature*, 1996, **381**, 212.
10. J. Lub, P. van de Witte, C. Doornkamp, J. P. A. Vogels and R. T. Wegh, *Adv. Mater.*, 2003, **15**, 1420; T. J. White, M. E. McConney and T. J. Bunning, *J. Mater. Chem.*, 2010, **20**, 9832; L. V. Natarajan, T. J. White, J. M. Wofford, V. P. Tondiglia, R. L. Sutherland, S. A. Siwecki and T. J. Bunning, *Appl. Phys. Lett.*, 2010, **97**, 11107.
11. A. C. Arsenault, T. J. Clark, G. von Freymann, L. Cademartiri, R. Sapienza, J. Bertolotti, E. Vekris, S. Wong, V. Kitaev, I. Manners, R. Z. Wang, S. John, D. Wiersma and G. A. Ozin, *Nat. Mater.*, 2006, **5**, 179; H. Masaki, S. Takahiro and T. Yukikazu, *Adv. Mater.*, 2009, **21**, 1801; J. Yoon, W. Lee and E. L. Thomas, *Macromolecules*, 2008, **41**, 4582; C. Kang, E. Kim, H. Baek, K. Hwang, D. Kwak, Y. Kang and E. L. Thomas, *J. Am. Chem. Soc.*, 2009, **131**, 7538; Y. J. Lu, H. W. Xia, G. Z. Zhang and C. Wu, *J. Mater. Chem.*, 2009, **19**, 5952.
12. M. George, V. A. Mallia, P. K. S. Antharjanam, M. Saminathan and S. Das, *Mol. Cryst. Liq. Cryst.*, 2000, **350**, 125; S. V. Serak, E. O. Arikainen, H. F. Gleeson, V. A. Grozhik, J. P. Guillou and N. A. Usova, *Liq. Cryst.*, 2002, **29**, 19; G. Wang, M. Zhang, T. Zhang, J. Guan and H. Yang, *RSC Adv.*, 2012, **2**, 487; Y. Li, M. Wang, A. Urbas and Q. Li, *J. Mater. Chem. C*, 2013, **1**, 3917.
13. Y. Kim, M. Wada and N. Tamaoki, *J. Mater. Chem. C*, 2014, **2**, 921; Y. Li, A. Urbas and Q. Li, *J. Org. Chem.*, 2011, **76**, 7148; R. A. van Delden, T. Mecca, C. Rosini and B. L. Feringa, *Chem. Eur. J.*, 2004, **10**, 61; H. Hattori and T. Uryu, *Liq. Cryst.*, 2001, **28**, 25; Y. Yokoyama and T. Sagisaka, *Chem. Lett.*, 1997, **26**, 687; S. Janicki, Z.; Schuster, G. B. *J. Am. Chem. Soc.*, 1995, **117**, 8524; T. J. White, R. L. Bricker, L. V. Natarajan, N. V. Tabiryan, L. Green, Q. Li and T. J. Bunning, *Adv. Funct. Mater.*, 2009, **19**, 3484.
14. R. P. Lemieux, *Soft Matter*, 2005, **1**, 348; H.-K. Lee, K. Doi, H. Harada, O. Tsutsumi, A. Kanazawa, T. Shiono and T. Ikeda, *J. Phys. Chem. B*, 2000, **104**, 7023; C. Ruslim and K. Ichimura, *J. Phys. Chem. B*, 2000, **104**, 6529.
15. Q. Hsu, Y. Wang, J. Jia, C. Wang, L. Feng, R. Dong, X. Sun and J. Hao, *Soft Matter*, 2012, **8**, 11492; X. Chen, L. Wang, C. Li, J. Xiao, H. ding, X. Liu, X. Zhang, W. He and H. Yang, *Chem. Commun.*, 2013, **49**, 10097.
16. L. A. Kutulya, G. P. Semenkova, N. I. Shkolnikova, V. V. Vashenko, L. L. Ostis, V. M. Sorokin and A. G. Kozachenko, *Mol. Cryst. Liq. Cryst.*, 2001, **357**, 43; K. Fukuda, H. Suzuki, J. Ni, M. Tokita and J. Watanabe, *Jpn. J. Appl. Phys.*, 2007, **46**, 5208; K. Fukuda, S. Edo, M. Muto, M. Tokita and J. Watanabe, *Jpn. J. Appl. Phys.*, 2008, **47**, 8479; N. I. Shkolnikova, L. A. Kutulya, N. S. Pivnenko, R. I. Zubatyuk and O. V. Shishkin, *Crystallogr. Rep.*, 2005, **50**, 1084; C.-H. Lin and C.-S. Hsu, *J. Polym. Res.*, 2000, **7**, 167.
17. D.-Y. Kim, S. Kim, S.-A Lee, Y.-E. Choi, W.-J. Yoon, S.-W. Kuo, C.-H. Hsu, M.-J. Huang, S. H. Lee and K.-U. Jeong, *J. Phys. Chem. C*, 2014, **118**, 6300; D.-Y. Kim, P. Nayek, S. Kim, K. S. Ha, M. H. Jo, C.-H. Hsu, Y. Cao, S. Z. D. Cheng, S. H. Lee and K.-U. Jeong, *Cryst. Growth. Des.*, 2013, **13**, 1309.
18. M. Mathews, R. S. Zola, D.-K. Yang and Q. Li, *J. Mater. Chem.*, 2011, **21**, 2098.
19. L. Green, Y. Li, T. J. White, A. Urbas, T. J. Bunning and Q. Li, *Org. Biomol. Chem.*, 2009, **7**, 3930
20. D.-Y. Kim, S.-A Lee, Y.-J. Choi, S.-H. Hwnag, S.-W. Kuo, C. Nah, M.-H. Lee and K.-U. Jeong, *Chem. Eur. J.*, 2014, **20**, 5689; D.-Y. Kim, S.-A Lee, H. J. Choi, L.-C. Chen, M.-H. Lee and K.-U. Jeong, *J. Mater. Chem. C*, 2013, **1**, 1375.
21. D.-Y. Kim, L. Wang, Y. Cao, X. Yu, S. Z. D. Cheng, S.-W. Kuo, D.-H. Song, S. H. Lee, M.-H. Lee and K.-U. Jeong, *J. Mater. Chem.*, 2012, **22**, 16382; N. Kim, L. Wang, D.-Y. Kim, S.-H. Hwang, S.-W. Kuo, M.-H. Lee and K.-U. Jeong, *Soft Matter*, 2012, **8**, 9183.
22. G. Ungar, J. L. Feijoo, V. Percec and R. Yourd, *Macromolecules*, **1991**, 24, 953; M. A. Yandrasits, S. Z. D. Cheng, A. Zhang, J. Cheng, B. Wunderlich and V. Percec, *Macromolecules*, 1992, **25**, 2112; K.-U. Jeong, B. S. Knapp, J. J. Ge, S. Jin, M. J. Graham, H. Xiong, F. W. Harris and S. Z. D. Cheng, *Macromolecules*, 2005, **38**, 8333.
23. D.-K. Yang, K.-U. Jeong and S. Z. D. Cheng, *J. Phys. Chem. B*, 2008, **112**, 1358; K.-U. Jeong, A. J. Jing, B. Monsdorf, J. Matthew, R. W. Harris and S. Z. D. Cheng, *J. Phys. Chem. C*, 2007, **111**, 767.
24. K.-U. Jeong, S. Jin, J. J. Ge, B. S. Knapp, M. J. Graham, J. Ruan, M. Guo, H. Xiong, F. W. Harris and S. Z. D. Cheng, *Chem. Mater.*, 2005, **17**, 2852; K.-U. Jeong, B. S. Knapp, J. J. Ge, S. Jin, M. J. Graham, F. W. Harris and S. Z. D. Cheng, *Chem. Mater.*, 2006, **18**, 680.
25. Y. Yoon, A. Zhang, R.-M. Ho and S. Z. D. Cheng, *Macromolecules*, 1996, **29**, 294; Y. Yoon, R.-M. Ho, B. Moon, D. Kim, K. W. McCreight, F. Li, F. W. Harris and S. Z. D. Cheng, *Macromolecules*, 1996, **29**, 3421.
26. Y. Huang, Y. Zhou, C. Doyle and S. T. Wu, *Opt. Express*, 2006, **14**, 1236; S. Furumi, S. Yokoyama, A. Otomo, and S. Mashiko, *Appl.*

Phys. Lett., 2004, **84**, 2491; P. G. de Gennes and J. Prost, *The Physics of Liquid Crystals*, Clarendon Press, Oxford, 1993.

27. J. Guo, H. Wu, F. Chen, L. Zhang, W. He, H. Yang and J. Wei, *J. Mater. Chem.*, 2010, **20**, 4094; R. M. Tejedor, L. Oriol, J. L. Serrano and T. Sierra, *J. Mater. Chem.*, 2008, **18**, 2899; A. Ryabchun, A. Bobrovsky, A. Sobolewska, V. Shibaev and J. Stumpe, *J. Mater. Chem.*, 2012, **22**, 6245.
28. W. Hu, H. Cao, L. Song, H. Zhao, S. Li, Z. Yang and H. Yang, *J. Phys. Chem. B.*, 2009, **113**, 13882; H. Yang, H. Kikuchi and T. Kajiyama, *Liq. Cryst.*, 2002, **29**, 1141; H. Yang, H. Kikuchi and T. Kajiyama, *Liq. Cryst.*, 2000, **27**, 1695; J. Geng, C. Dong, L. Zhang, Z. Ma, L. Shi, H. Cao and H. Yang, *Appl. Phys. Lett.*, 2006, **89**, 81130; F. Ania and H. Stegemeyer, *Mol. Cryst. Liq. Cryst. Lett. Sect.*, 1985, **2**, 67; N. I. Shkolnikova, L. A. Kutulya, N. S. Pivnenko, R. I. Zubatyuk and O. V. Shishkin, *Crystallogr. Rep.*, 2005, **50**, 1005; X. Yuan, L. Zhang and H. Yang, *Liq. Cryst.*, 2010, **37**, 445; Z. Cheng, K. Li, R. Guo, F. Wang, X. Wu, L. Zhang, J. Xiao, H. Cao, Z. Yang and H. Yang, *Liq. Cryst.*, 2011, **38**, 233.
29. S. S. Choi, S. M. Morris, W. T. S. Huck and H. J. Coles, *Adv. Mater.*, 2009, **21**, 3915; C. A. Bailey, V. P. Tondiglia, L. V. Natarajan, M. M. Duning, R. L. Bricker, R. L. Sutherland, T. J. White, M. F. Durstock and T. J. Bunning, *J. Appl. Phys.*, 2010, **107**, 013105; V. T. Tondiglia, L. V. Natarajan, C. A. Bailey, M. M. Duning, R. L. Sutherland, D.-K. Yang, A. Voevodin, T. J. White and T. J. Bunning, *J. Appl. Phys.*, 2011, **110**, 053109.
30. M. Z. Alam, T. Yshioka, T. Ogata, T. Nanaka and S. Kurihara, *Chem. Eur. J.*, 2007, **13**, 2641; T. Yoshioka, T. Ogata, T. Nonaka, M. Moritsugu, S.-N. Kim and S. Kurihara, *Adv. Mater.*, 2005, **17**, 1226.
31. J. Ma, Y. Li, T. J. White, A. Urbas and Q. Li, *Chem. Commun.*, 2010, **46**, 3463; M. Mathews and N. Tamaoki, *J. Am. Chem. Soc.*, 2008, **130**, 11409.
32. D. J. Broer, J. Lub and G. N. Mol, *Nature*, 1995, **378**, 467; D. J. Broer, G. N. Mol, J. A. M. M. van Haaren and J. Lub, *Adv. Mater.*, 1999, **11**, 573; X. Chen, L. Wang, Y. Chen, C. Li, G. Hou, X. Liu, X. Zhang, W. He and H. Yang, *Chem. Commun.*, 2014, **50**, 691; B. Fan, S. Vartak, J. N. Eakin and S. M. Faris, *Appl. Phys. Lett.*, 2008, **92**, 61101.

